Validation for SGLI/GCOM-C ocean color products in the coastal waters of Hokkaido

T. Isada[1], S. B. Hooker[2], J. W. Brown[3], Y. Taniuchi[4], K. Suzuki[1]
([1]Hokkaido Univ., Japan, [2]NASA/GSFC, USA, [3]University of Miami, USA, [4]FRA, Japan)

Summary

Coastal ecosystems are important in biogeochemical cycles, because they provide many pathways for chemical elements and compounds to flow between the physical environment and living organisms. The spatial and temporal scales of the biotic and abiotic interactions establish the inherent dynamics of the coastal zone and the requirement for high-resolution investigations. Using match-up data collected in Hokkaido coastal waters, the study herein evaluated the performance of deriving chlorophyll (Chl) *a* concentration and colored dissolved organic matter (CDOM) absorption (a_{CDOM}) as a function of wavelength (λ) from satellite observations. The Japanese Aerospace Exploration Agency (JAXA) Second generation GLobal Imager (SGLI), which has 250 m spatial resolution, was compared with other satellite ocean color (OC) sensors. Our results show that the standard SGLI OC4 algorithm with the 530 nm band provided the best performance for Chl *a* retrievals, and the end-member analysis (EMA) technique improved the estimation of $a_{CDOM}(\lambda)$. Overall differences between *in situ* radiometric data and satellite retrievals suggest that additional challenges remain, especially in the ultraviolet and blue spectral domains which are useful for studying CDOM and harmful algae blooms in coastal waters. To fulfil applications wherein high quality remote sensing data are required, the improvement of the atmospheric correction is a likely research area where additional accomplishment will be beneficial for satellite observations of optically complex coastal waters.

Field campaigns and sample analysis

In situ sample and data collection

In situ remote sensing reflectance (R_{rs}), Chl *a*, and CDOM data were collected in the Japanese coastal waters around the island of Hokkaido (Fig. 1A) with the highest data density obtained in Akkeshi Bay (Fig. 1B) from 2016 to 2020.

Sample analysis

1. $E_s(\lambda)$, $E_d(\lambda)$, $L_u(\lambda)$ (Hooker *et al.*, 2010)
   Instrument: SuBOPS (Biospherical Instruments, Inc.)
2. $a_{CDOM}(\lambda)$ (Babin *et al.*, 2003)
   Instrument: Spectrophotometer (UV-2600, Shimadzu),
3. Chlorophylls and carotenoids (Welschmeyer 1994, Suzuki *et al.*, 2015)
   Instrument: Turner Designs fluorometer (model 10-AU) and UHPLC (Nexera *X2*, Shimadzu)

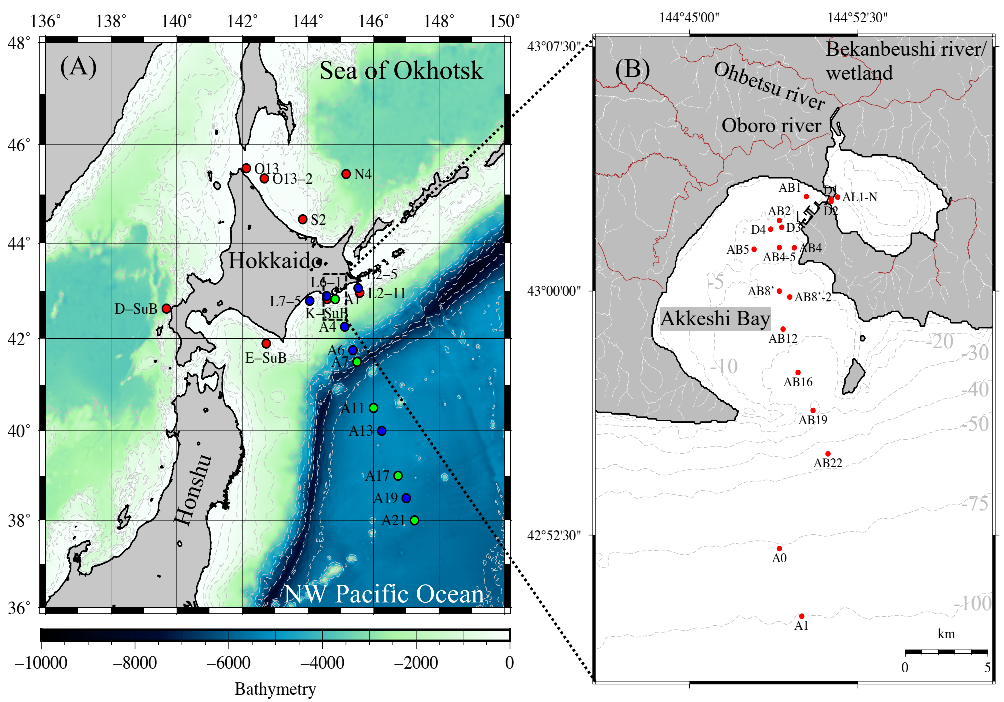

Figure 1. Observation sites in (A) the coastal waters around Hokkaido and (B) Akkeshi Bay, Japan. Closed green, blue, and red symbols in (A) represent the stations during HK1601, HK1610, and HK1810 field campaigns aboard the FR/V Hokko Maru (FRA), respectively.

Assessment of $R_{rs}(\lambda)$ and Chl *a* derived from satellite observations – match-up analysis

- We evaluated the performance of deriving $R_{rs}(\lambda)$, Chl *a* concentration and CDOM from satellite observations.
- The SGLI OC4 algorithm with the 530 nm band provided the best performance for Chl *a* retrievals.

$R_{rs}(\lambda)$ match-up data analysis

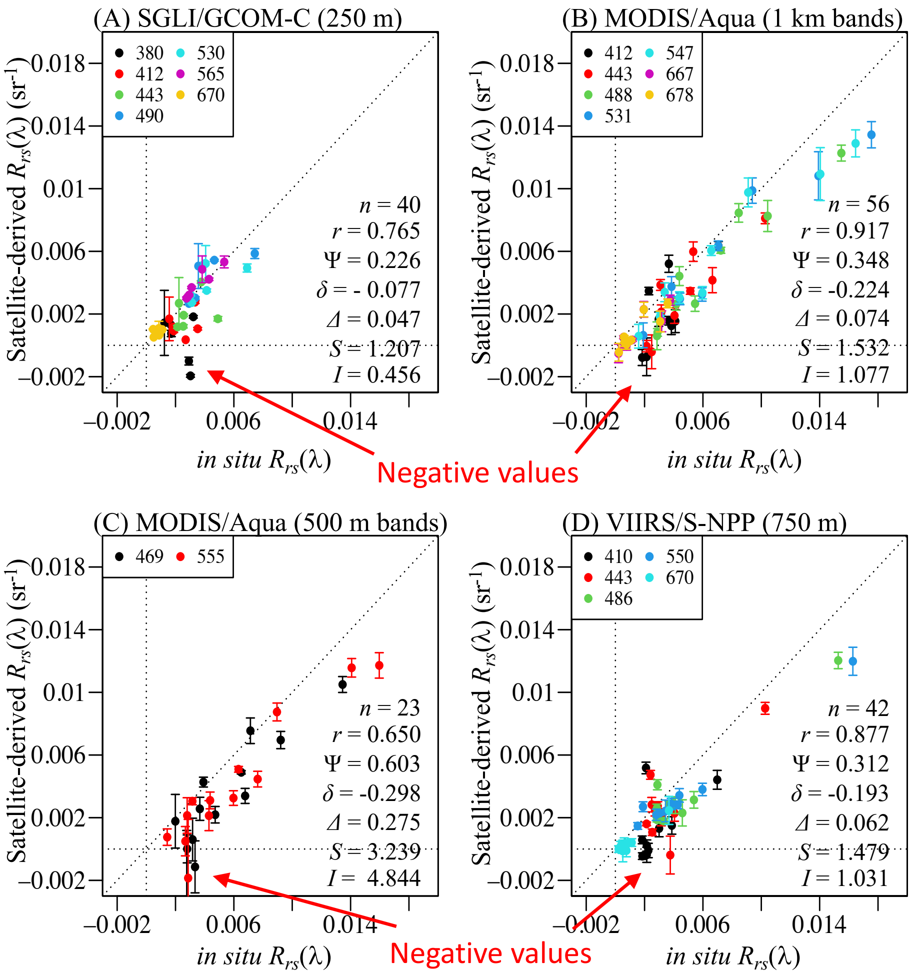

Figure 2. Scatter plots of *in situ* $R_{rs}(\lambda)$ versus $R_{rs}(\lambda)$ derived from (A) SGLI/GCOM-C, (B) MODIS/Aqua with 1 km resolution bands, (C) MODIS/Aqua with 500 m bands, and (D) VIIRS/Suomi-NPP. The horizontal, vertical, and diagonal dashed lines represent the zero coordinates of the X and Y axes and the 1:1 straight lines, respectively.

Chl *a* match-up data analysis

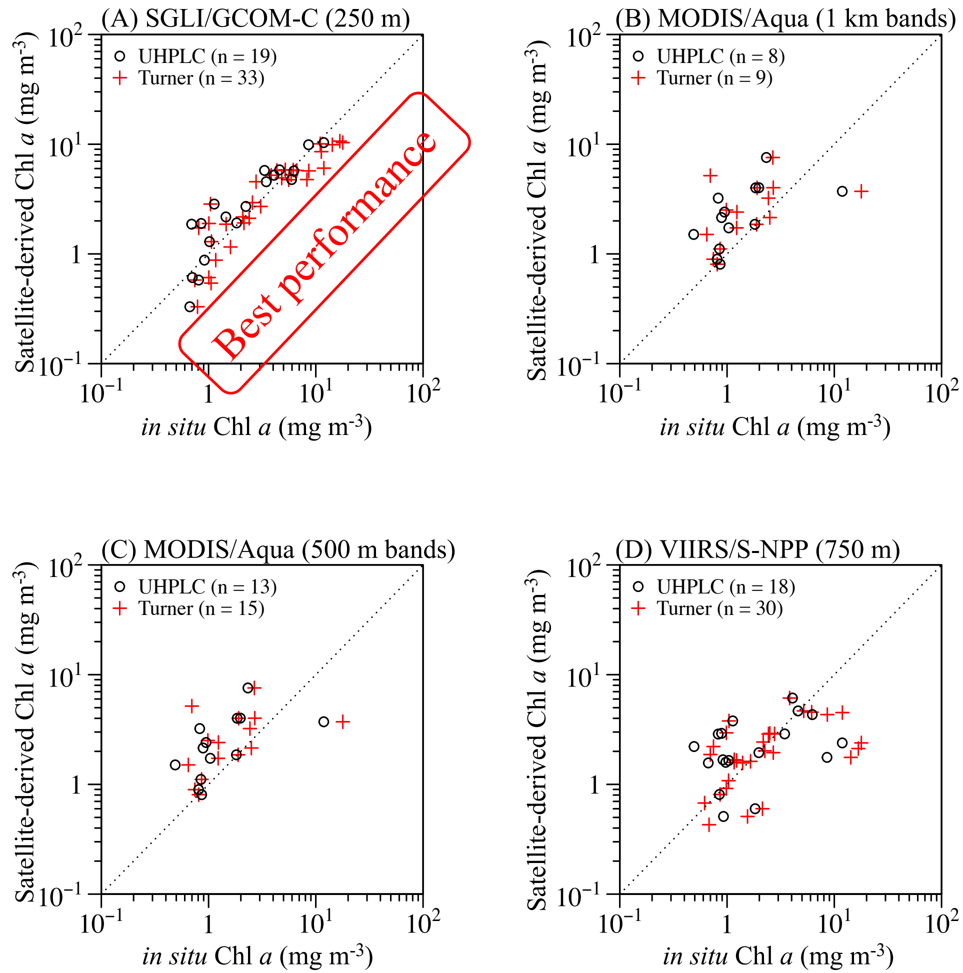

Figure 3. Scatter plots of *in situ* UHPLC- and Turner-derived Chl *a* concentrations versus Chl *a* concentrations derived from (A) SGLI/GCOM-C, (B) MODIS/Aqua with 1 km resolution bands, (C) MODIS/Aqua with 500 m bands, and (D) VIIRS/Suomi-NPP. The dashed lines represent the 1:1 straight line.

Development of local end-member analysis (EMA) for the retrieval of CDOM from satellite

The end-member analysis (EMA) technique improved the estimation of $a_{CDOM}(\lambda)$.

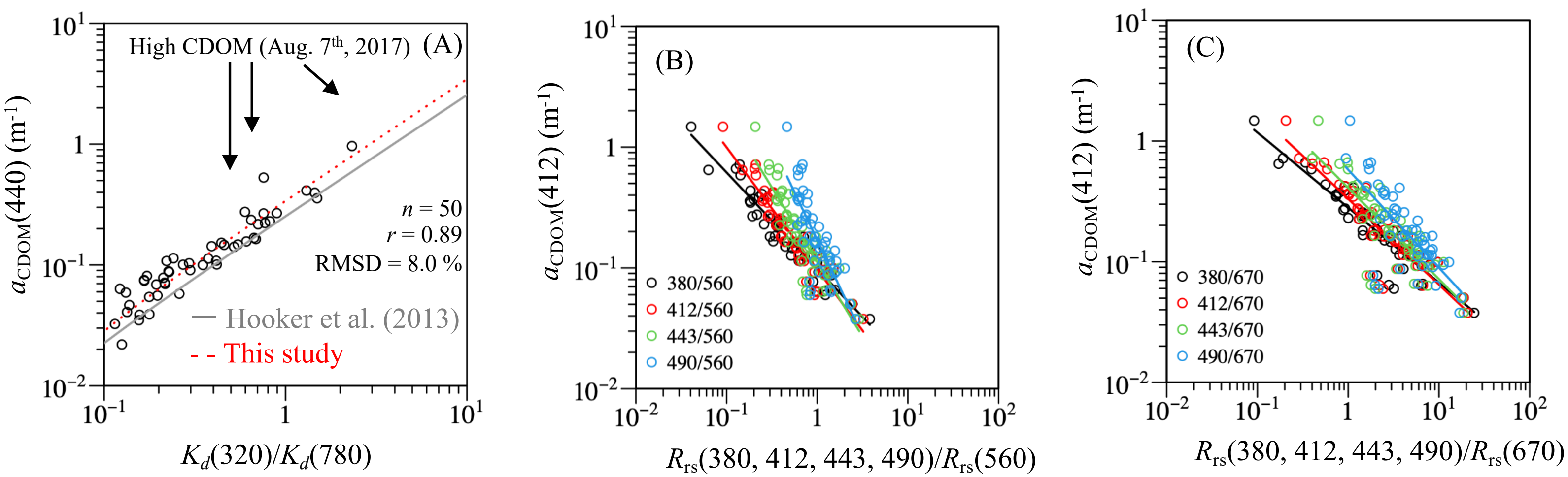

Figure 4. Field measurement-based relationships (A) between $a_{CDOM}(440)$ and $K_d(380)/K_d(780)$ and of $a_{CDOM}(412)$ with (B) $R_{rs}(\lambda)/R_{rs}(560)$ and (C) $R_{rs}(\lambda)/R_{rs}(670)$ at 380, 412, 443, and 490 nm, respectively.

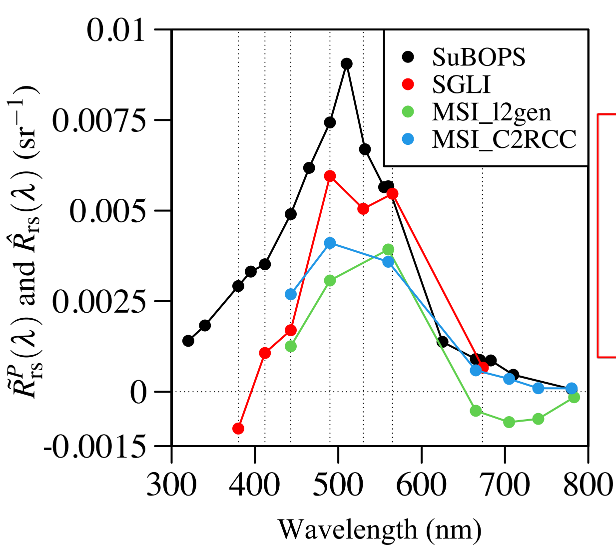

The improvement and development of the atmospheric correction would be required.

Figure 5. Spectral $R_{rs}(\lambda)$ performance comparison of *in situ* radiometric measurement with SuBOPS, SGLI/GCOM-C, and MSI/Sentinel2B with NIR-SWIR (l2gen) and C2RCC on 11 December 2019. The vertical dashed lines represent the SGLI bands.

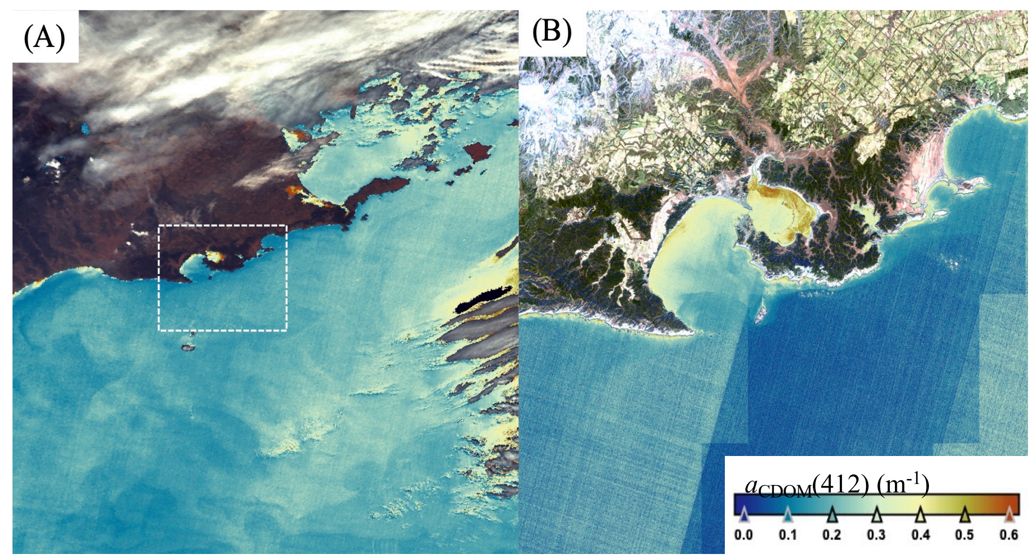

Figure 6. (A) SGLI/GCOM-C-derived and (B) MSI/Sentinel 2A (C2RCC) – derived $a_{CDOM}(412)$ based on the two end-member algorithm for Akkeshi Bay on 11 December 2019.

Isada et al. (submitted to the special issue on SGLI/GCOM-C of Journal of Oceanography)